Electronic Supplementary Material (ESI) for Catalysis Science & Technology.

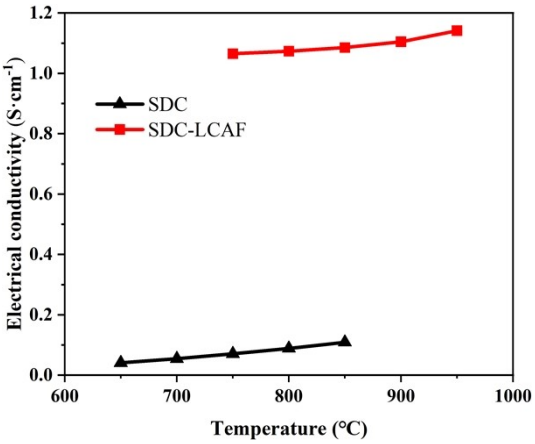

Fig. S1 Electrical conductivity of SDC and SDC-LCAF membrane materials in air atmosphere as a function of temperature.

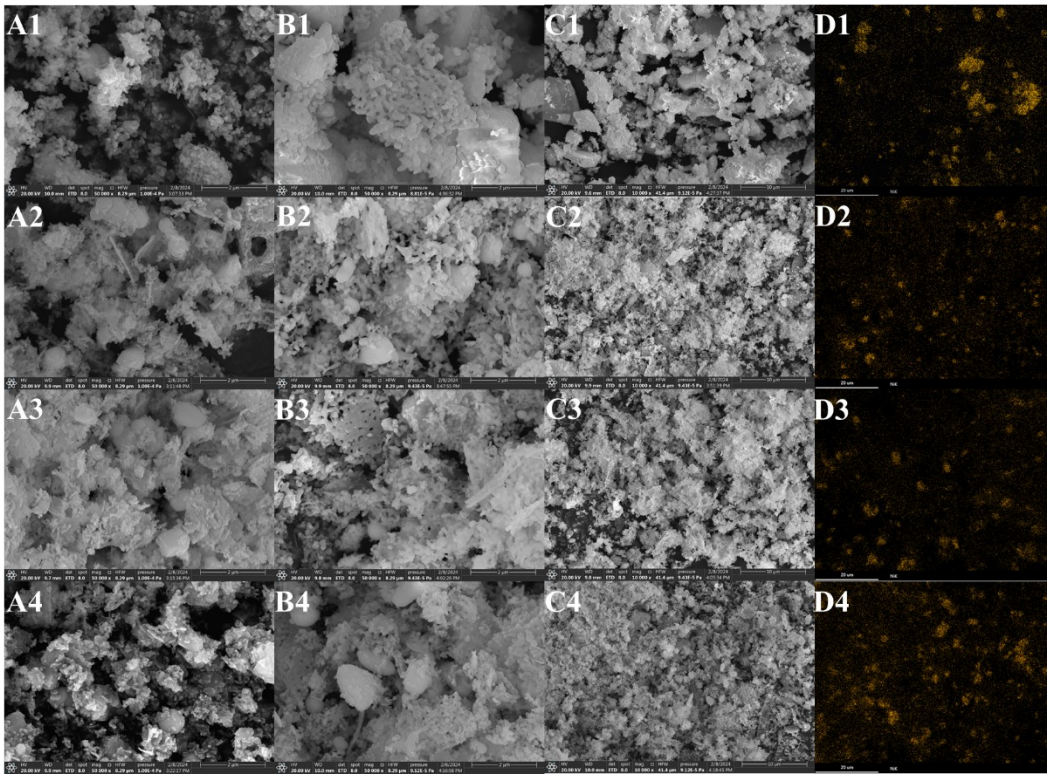

Fig. S2 (A-C) Morphology of NiO/SDC-LCAF catalyst with different Ni content before and after hydrogen reduction, (D) Ni distribution patterns of Fig. C (A, before reduction; B and C after reduction. 1, 10 wt.%; 2, 20 wt.%; 3, 30 wt.%; 4, 40 wt.%).

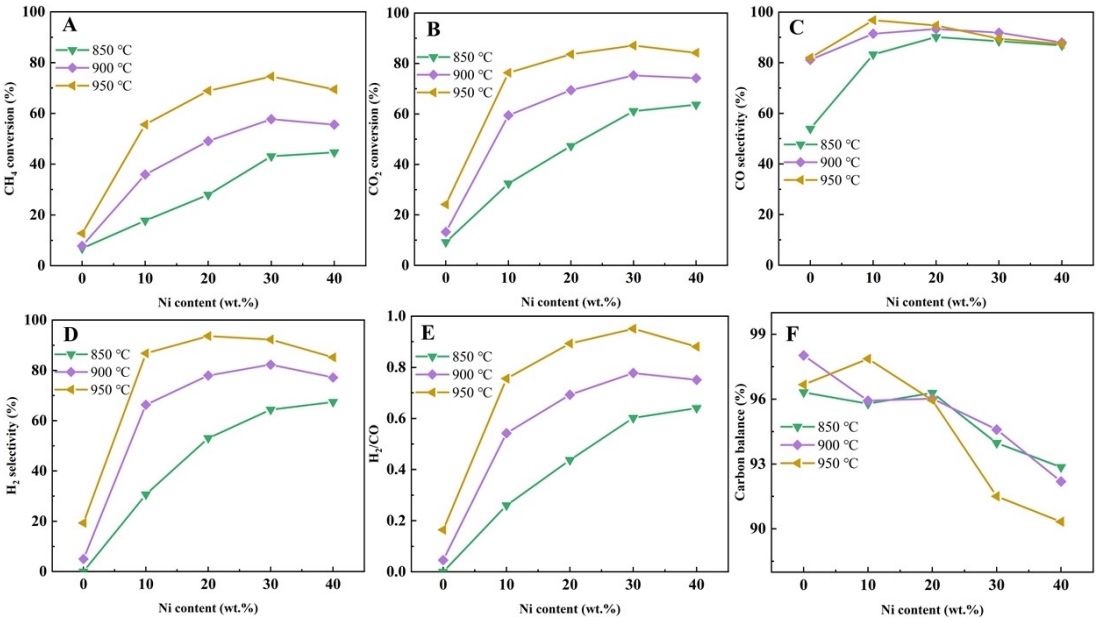

Fig. S3 DRM catalytic performance of catalysts with different Ni contents: (A) CH_4 and (B) CO_2 conversion, (C) CO and (D) H_2 selectivity, (E) H_2/CO molar ratio, and (F) carbon balance (feed gas was 50 mL min^{-1} CH_4 and 50 mL min^{-1} CO_2).

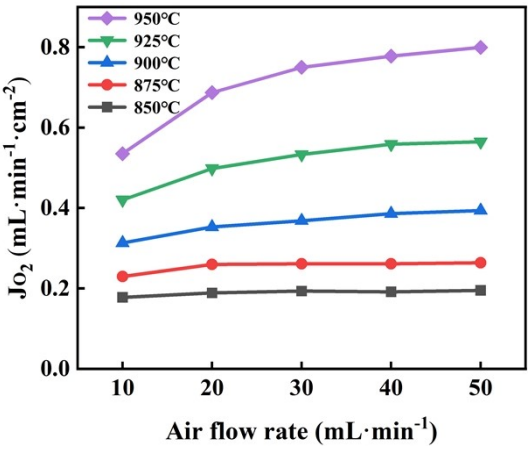

Fig. S4 Oxygen permeation fluxes of SDC-LCAF hollow fiber membrane at different air feed flow rates (900 °C, He sweep flow rate was 100 mL min^{-1}).

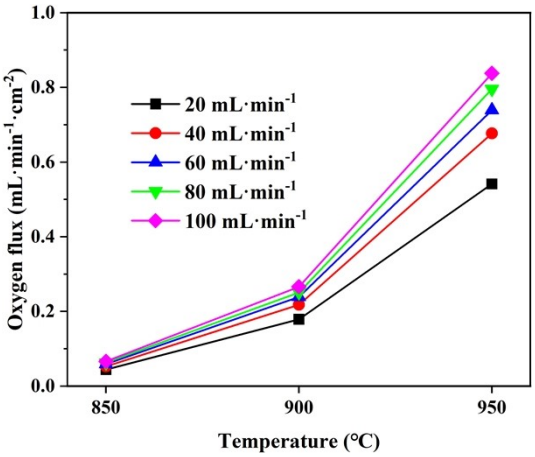

Fig. S5 Effect of He sweep flow rate on oxygen flux of LCAF-SDC hollow fiber membrane as a function of temperature (Air feed flow rate was 100 mL min^{-1}).

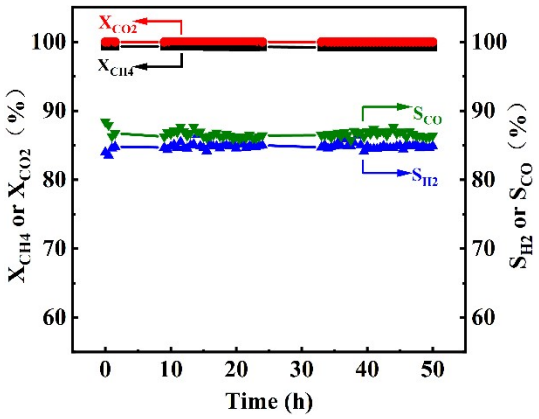

Fig. S6 DRM stability of SDC-LCAF HFM reactor at 900 ℃ (flow rate of CH_4-CO_2-He was 10-10-20 mL min^{-1}, respectively).

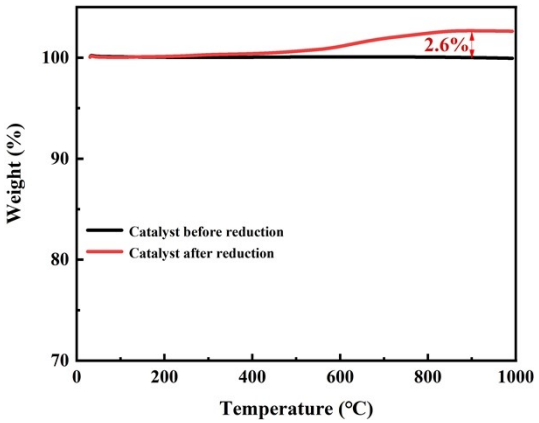

Fig. S7 TGA curves of catalysts before and after reduction.

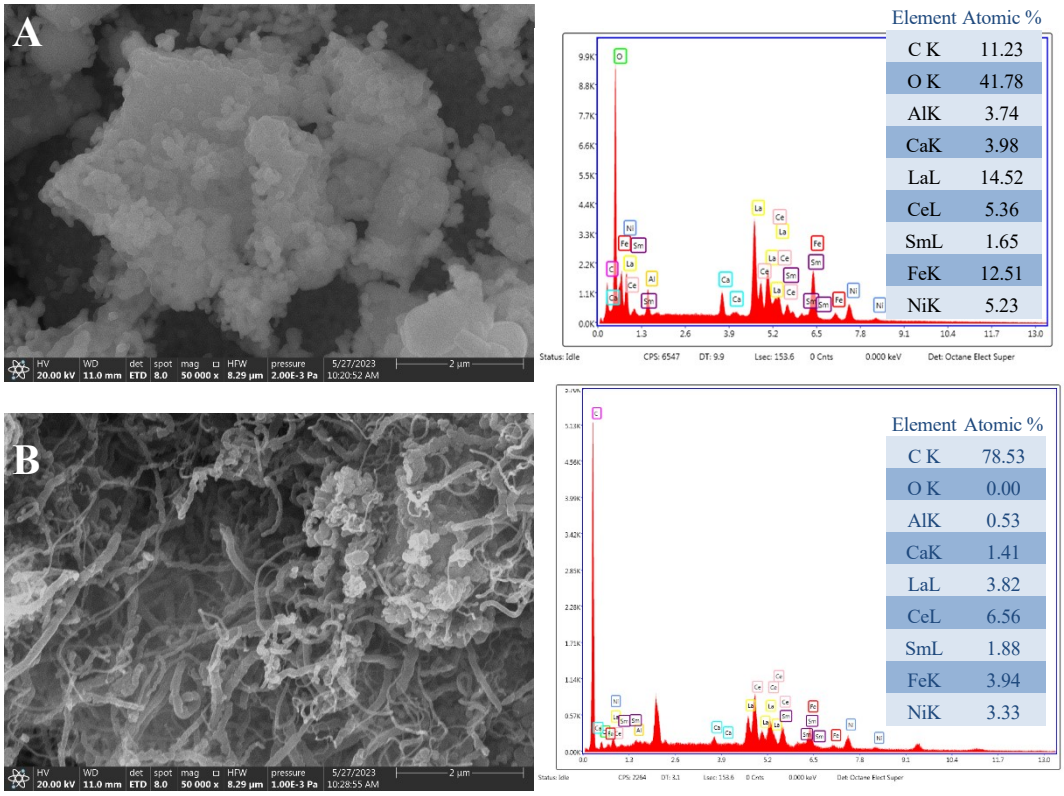

Fig. S8 EDS mapping of spent catalysts after (A) OCRM and (B) DRM.